Quantum Opt. 3 (1991) 221–237. Printed in the UK

Number and phase quantum fluctuations in second harmonic generation

R Tanaś†, Ts Gantsog‡ and R Zawodny†

Laboratory of Theoretical Physics, Joint Institute for Nuclear Research, Dubna, Head Post Office PO Box 79, Moscow 101000, USSR

Received 14 February 1991, in final form 8 April 1991

Abstract. Photon number and phase fluctuations and correlations in the second harmonic generation are discussed. The new Pegg–Barnett Hermitian phase formalism is used to deal with the phase properties of the field. The method of numerical diagonalization of the interaction Hamiltonian is applied to find the state evolution and, consequently, the number and phase quantum fluctuations. It is shown that the joint phase probability distribution evolves into a multi-peak structure indicating clearly the transition from the second harmonic to the down-conversion regime, and back. The evolution of all relevant quantities is illustrated graphically, and their dependence on the mean number of photons of the initial field is shown explicitly. The number–phase uncertainty product for the fundamental mode is plotted making evident the abrupt transition from the low to the high level of quantum fluctuations.

1. Introduction

Second harmonic generation which was observed in the early days of lasers [1] is perhaps the simplest non-linear optical process. Due to its simplicity and variety of practical applications the second harmonic generation is a starting point for presenting non-linear optical processes in the textbooks on non-linear optics (see for example [2, 3]). Classically, the second harmonic generation means the appearance of the field at frequency 2ω (second harmonic) when the optical field of frequency ω (fundamental mode) propagates through a non-linear crystal. In the quantum picture of the process we deal here with a non-linear process in which two photons of the fundamental mode are annihilated and one photon of the second harmonic is created. The classical treatment of the problem allows closed form solutions with the possibility of energy being transferred completely into the second harmonic mode. For quantum fields, the closed form analytical solution of the problem has not been found unless some approximations are made. The early numerical solutions [4] showed that quantum fluctuations of the field prevent the complete transfer of energy into the second harmonic and the solutions become oscillatory. Later studies showed that the quantum states of the field generated in the process have a number of unique quantum

† Permanent address: Nonlinear Optics Division, Institute of Physics, Adam Mickiewicz University, 60-780 Poznań, Poland.

‡ Permanent address: Department of Theoretical Physics, Mongolian State University, Ulan Bator 210646, Mongolia.

0954-8998/91/040221+17$03.50 © 1991 IOP Publishing Ltd

features such as photon antibunching [5] and squeezing [6, 7] for both fundamental and second harmonic modes (for a review and literature on quantum effects see [8]).

Recently, Nikitin and Masalov [9] have discussed properties of the quantum state of the fundamental mode calculating numerically the quasiprobability distribution function $Q(\alpha, \alpha^*)$ for this mode. They have suggested that the quantum state of the fundamental mode evolves, in the course of the second harmonic generation, into a superposition of two macroscopically distinguishable states. Such superpositions of well separated coherent states that appear in the evolution of an anharmonic oscillator [10] are clearly indicated by the splitting of the Q function into separate peaks [11]. As Gantsog and Tanaś [12, 13] have recently shown using the new Pegg–Barnett [14–16] Hermitian phase formalism, such superpositions are also clearly visible in the phase distribution functions.

In this paper we consider the problem of photon number and phase quantum fluctuations and correlations in the field produced by the second harmonic generation process. The fully quantum approach using the method of numerical diagonalization of the interaction Hamiltonian [17, 18] is employed for getting the evolution of the system. The evolution of the photon number fluctuation in both fundamental and second harmonic modes, the correlation between the numbers of photons of the two modes, the joint phase probability distribution, the phase variances for the two modes, the intermode phase correlation, and the number–phase uncertainty product are obtained and illustrated graphically. Some of the results for photon number fluctuations in particular modes of the field are known [4, 18], but are reproduced here to contrast them with the new results for the phase fluctuations and correlations. To describe the phase properties of the field the new Pegg–Barnett [14–16] Hermitian phase formalism is used. A qualitative change in the phase distribution, a transition from a one-peak into a two-peak structure (a sort of 'phase transition') is found to appear during the evolution. A sequence of such 'bifurcations' leads eventually (in the long time limit) to the randomization of the phase.

2. Quantum evolution of the field state

The second harmonic generation process is described by the following model Hamiltonian

$$H = H_0 + H_{\mathrm{I}} = \hbar\omega a^\dagger a + 2\hbar\omega b^\dagger b + \hbar g(b^\dagger a^2 + b a^{\dagger 2}) \tag{1}$$

where a ($a^\dagger$) and b ($b^\dagger$) are the annihilation (creation) operators of the fundamental mode of frequency ω and the second harmonic mode of frequency 2ω, respectively. The coupling constant g, which is real, describes the coupling between the two modes. The same Hamiltonian describes the reverse process of sub-harmonic generation (or the parametric down-conversion with quantum pump). The difference between the two processes is in the initial conditions. The second harmonic generation takes place when the mode of frequency ω is initially populated and the mode at frequency 2ω is in the vacuum. In the case of sub-harmonic generation the initial population of the two modes is interchanged.

Since H_0 and H_{I} commute, there are two constants of motion: H_0 and H_{I}. H_0 determines the total energy stored in both modes, which is conserved by the interaction H_{I}. This allows us to factor out $\exp(-\mathrm{i}H_0 t/\hbar)$ from the evolution

operator and, in fact, to drop it altogether. In effect, the resulting state of the field can be written as

$$|\Psi(t)\rangle = \exp(-\mathrm{i}H_{\mathrm{I}}t/\hbar)|\Psi(0)\rangle \tag{2}$$

where $|\Psi(0)\rangle$ is the initial state of the field. If the Fock states are used as basis states, the interaction Hamiltonian H_{I} is not diagonal in such a basis. To find the state evolution, we apply the numerical method of diagonalization of H_{I} [17, 18].

Let us assume that initially there are n photons in the fundamental mode and no photons in the second harmonic mode, i.e., the initial state of the field is $|n,0\rangle = |n\rangle|0\rangle$. Since H_0 is a constant of motion, we have the relation

$$\langle a^\dagger a\rangle + 2\langle b^\dagger b\rangle = \mathrm{constant} = n \tag{3}$$

which implies that the creation of k photons of the second harmonic mode requires annihilation of $2k$ photons of the fundamental mode. Thus, for given n, we can introduce the states

$$|\psi_k^{(n)}\rangle = |n-2k,k\rangle \qquad k = 0,1,\ldots,[n/2] \tag{4}$$

where $[n/2]$ means the integer part of $n/2$, which form a complete basis of states of the field for given n. We have

$$\langle\psi_{k'}^{(n')}|\psi_k^{(n)}\rangle = \delta_{nn'}\delta_{kk'} \tag{5}$$

which means that the constant of motion H_0 splits the field space into orthogonal subspaces, which for given n have the number of components equal to $[n/2]+1$. In such a basis the interaction Hamiltonian has the following non-zero matrix elements

$$\begin{aligned}\langle\psi_{k+1}^{(n)}|H_{\mathrm{I}}|\psi_k^{(n)}\rangle &= \langle\psi_k^{(n)}|H_{\mathrm{I}}|\psi_{k+1}^{(n)}\rangle = (H_{\mathrm{I}})_{k+1,k}^{(n)} = (H_{\mathrm{I}})_{k,k+1}^{(n)}\\ &= \hbar g\sqrt{(k+1)(n-2k)(n-2k-1)}\end{aligned} \tag{6}$$

which form a symmetric matrix of dimension $([n/2]+1)\times([n/2]+1)$ with real non-zero elements (we have assumed g real) that are located on the two diagonals immediately above and below the principal diagonal. Such a matrix can be easily diagonalized numerically [17].

To find the state evolution, we need the matrix elements of the evolution operator

$$c_{n,k}(t) = \langle\psi_k^{(n)}|\exp(-\mathrm{i}H_{\mathrm{I}}t/\hbar)|\psi_0^{(n)}\rangle. \tag{7}$$

If the matrix U is the unitary matrix that diagonalizes the interaction Hamiltonian matrix given by equations (6), i.e.,

$$U^{-1}H_{\mathrm{I}}^{(n)}U = \hbar g \times \mathrm{diag}\left(\lambda_0,\lambda_1,\ldots,\lambda_{[n/2]}\right) \tag{8}$$

then the coefficients $c_{n,k}(t)$ can be written as

$$c_{n,k}(t) = \sum_{i=0}^{[n/2]} \mathrm{e}^{-\mathrm{i}gt\lambda_i}U_{ki}U_{0i}^* \tag{9}$$

where λ_i are the eigenvalues of the interaction Hamiltonian in units of $\hbar g$. Of course, the matrix U as well as the eigenvalues λ_i are defined for given n and should have the additional index n, which we have omitted to shorten the notation. Moreover, for real g the interaction Hamiltonian matrix is real, and the transformation matrix U is a real orthogonal matrix, so the star can also be dropped.

The numerical diagonalization procedure gives the eigenvalues λ_i as well as the elements of the matrix U, and the coefficients $c_{n,k}(t)$ can thus be calculated according to (9). It is worthwhile to notice, however, that due to the symmetry of the Hamiltonian the eigenvalues λ_i are distributed symmetrically with respect to zero, with one eigenvalue equal to zero if there is an odd number of them. When the eigenvalues are numbered from the lowest to the highest value, there is an additional symmetry relation

$$U_{ki}U_{0i} = (-1)^k U_{k,[n/2]-i}U_{0,[n/2]-i} \tag{10}$$

which makes the coefficients $c_{n,k}(t)$ either real (k even) or imaginary (k odd). This property of the coefficients $c_{n,k}(t)$ is very important and allows in some cases to get exact analytical results.

Knowing the coefficients $c_{n,k}(t)$ the resulting state of the field (2) can be written, for the initial state $|n,0\rangle$, as

$$|\psi^{(n)}(t)\rangle = \sum_{k=0}^{[n/2]} c_{n,k}(t)|\psi_k^{(n)}\rangle. \tag{11}$$

The typical initial conditions for the second harmonic generation are a coherent state of the fundamental mode and the vacuum of the second harmonic mode. The initial state of the field can thus be written as

$$|\psi(0)\rangle = \sum_{n=0}^{\infty} b_n|n,0\rangle \tag{12}$$

where

$$b_n = \exp(N_a/2)\frac{N_a^{n/2}}{\sqrt{n!}}\mathrm{e}^{\mathrm{i}n\varphi_a} \tag{13}$$

is the Poissonian weighting factor of the coherent state $|\alpha\rangle$ represented as a superposition of the number states, $N_a = |\alpha|^2$ is the mean number of photons, and φ_a is the phase of the coherent state – $\alpha = \sqrt{N_a}\exp(\mathrm{i}\varphi_a)$. With these initial conditions the resulting state (2) is given by

$$|\psi(t)\rangle = \sum_{n=0}^{\infty} b_n|\psi^{(n)}(t)\rangle = \sum_{n=0}^{\infty} b_n \sum_{k=0}^{[n/2]} c_{n,k}(t)|n-2k,k\rangle. \tag{14}$$

Equation (14) describing the evolution of the system is our starting point for further discussion of the second harmonic generation. If the initial state of the fundamental mode is not a coherent state, but it has a decomposition into the number states of the form (12) with different amplitudes b_n, equation (14) is still valid when corresponding b_n are taken. It is true, for example, for the initially squeezed state of the fundamental mode.

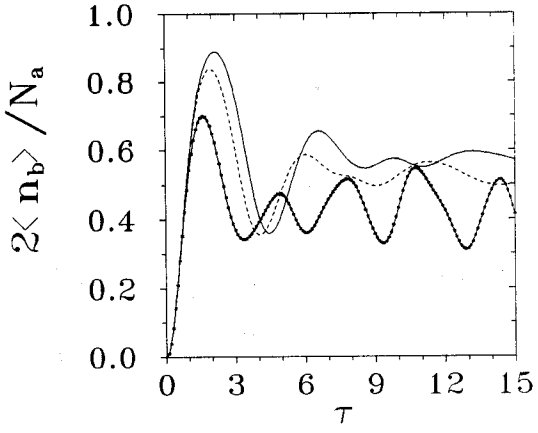

Figure 1. Plots of $2\langle n_b\rangle/N_a$ against the scaled time $\tau = \sqrt{2N_a}gt$, for $N_a = 4$ (bold curve), $N_a = 16$ (broken curve), and $N_a = 36$ (full curve). The same description of the curves is used in other figures.

3. Photon numbers evolution: expectation values, fluctuations and correlations

The classical solution for the second harmonic intensity (see for example [13]), for perfect phase-matching and absence of the second harmonic for $t = 0$, can be, in our notation, written as

$$\langle n_b\rangle_{\text{class}} = \frac{N_a}{2}\tanh^2\left(\sqrt{2N_a}gt\right). \tag{15}$$

This solution means the monotonic growth of the second harmonic intensity and asymptotically a complete power transfer to the second harmonic mode.

It is well known [4, 18], however, that the quantum solution has oscillatory character and does not allow for the complete power transfer. Since the closed-form analytical solution is not available in the quantum case, one has to use some approximations or numerical methods to find the solution. Using the state (14), the mean number of photons of the second harmonic evolves according to the formula

$$\langle n_b\rangle = \langle\psi(t)|b^\dagger b|\psi(t)\rangle = \sum_{n=0}^{\infty}|b_n|^2\sum_{k=0}^{[n/2]}k|c_{n,k}(t)|^2. \tag{16}$$

Because of the Poissonian factors, which are peaked at N_a, the summation (16) can be performed numerically if N_a is not too great. On the other hand, some features of the classical solution can be expected for $N_a \gg 1$. We evaluate numerically formula (16) to find the evolution of the mean number of photons of the second harmonic mode for $N_a = 4$, 16 and 36. The results are shown in figure 1, where $2\langle n_b\rangle/N_a$ is plotted against the scaled time $\tau = \sqrt{2N_a}gt$. Such scaling of time is prompted by the classical solution (15) and sets a proper time-scale when various N_a are considered. The oscillatory behaviour discussed earlier [4, 18] is clearly visible. The oscillations decay faster for higher N_a. The fraction of energy that is transferred to the second harmonic increases as N_a increases, and for $N_a = 36$ the maximum transfer is about 90 per cent. Of course, due to energy conservation we have $\langle n_a\rangle + 2\langle n_b\rangle = N_a$.

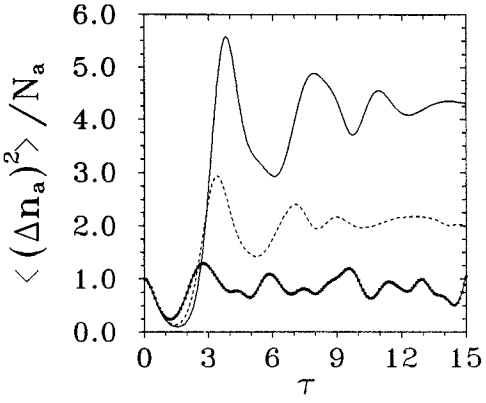

Figure 2. Evolution of the relative number fluctuations for the fundamental mode.

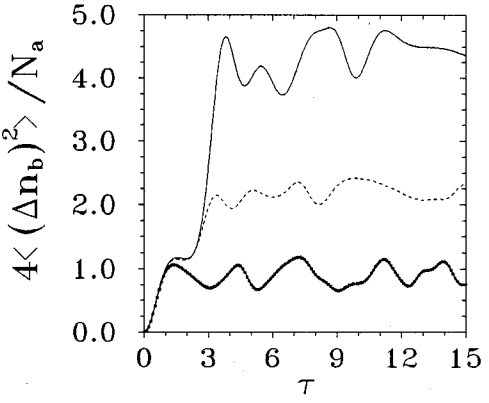

Figure 3. Same as figure 2 but for the second harmonic mode.

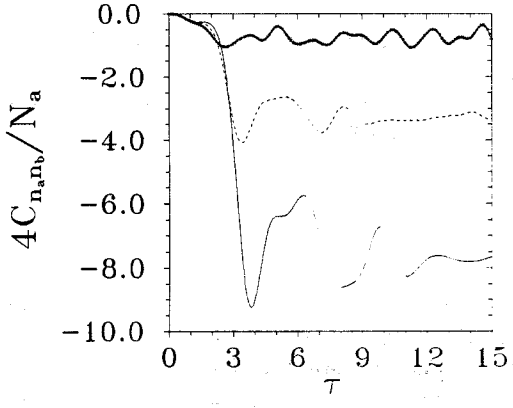

Figure 4. Evolution of the intermode number correlations.

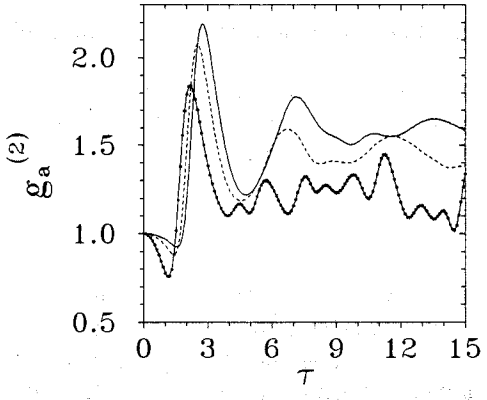

Figure 5. Plots of the $g^{(2)}$ function for the fundamental mode.

Since H_0 is a constant of motion, H_0^2 is also a constant of motion, which gives for the fluctuations of H_0 the following relation

$$\langle(\Delta H_0)^2\rangle = \langle H_0^2\rangle - \langle H_0\rangle^2 = N_a(\hbar\omega)^2 \tag{17}$$

and this can be rewritten as

$$\langle(\Delta n_a)^2\rangle + 4\langle(\Delta n_b)^2\rangle + 4\langle\Delta n_a \Delta n_b\rangle = N_a. \tag{18}$$

Formula (18) establishes the relation between the fluctuations of the individual-mode photon numbers and the intermode photon-number correlation. All the quantities on the left hand side of (18) can be calculated numerically using the state (14), and formula (18) can serve as a test of numerical precision. N_a sets the level of fluctuations for an initially coherent state. The evolution of relative fluctuations and correlations is shown in figures 2–4, for $N_a = 4$, 16 and 36. It is seen that after the

maximum of the second harmonic has been passed ($\tau \approx 2$) there is a rapid growth of photon fluctuations in both modes, which is compensated by the negative correlation $C_{n_a n_b} = \langle \Delta n_a \Delta n_b \rangle$. In the long time limit the relative fluctuations become close to certain values, which are larger for larger N_a. Since the photon statistics in the second harmonic have already been discussed [4] and the non-classical character of the field states proved [5–9, 18], we are not going to give here any extensive discussion of those problems. Just for easier comparisons we show in figure 5 plots of the $g^{(2)}$ function for the fundamental mode ($g_a^{(2)} = \langle n_a(n_a - 1)\rangle / \langle n_a \rangle^2$). Initially photon statistics are sub-Poissonian, but the effect is smaller for large N_a. Next, there is a sharp increase of $g_a^{(2)}$, and the super-Poissonian peak occurs. This peak is associated with squeezing in the fundamental mode. In the long time limit $g_a^{(2)}$ approaches its asymptotical values that depends on N_a. Beside the photon statistics in the individual modes, we would like to emphasize the fact of strong negative correlation between the photon-number fluctuations of the two modes, which is associated with the rapid growth of the photon-number fluctuations in each mode. This transition from the state with low fluctuations (and correlations) to the state with high fluctuations (and correlations) means the qualitative change of the field state, and can be associated with the transition of the process from the second harmonic to the down-conversion regime when the maximum of the second harmonic intensity has been passed. In fact, there is a competition between the two processes all the time, and only initially can one safely speak about 'pure' second harmonic generation. The qualitative change of the field state is much more spectacular when the phase properties of the field are considered.

4. Phase properties of the field

To study phase properties of the field obtained in the second harmonic generation process, we use the new Pegg and Barnett [14–16] phase formalism which is based on introducing a finite $(s+1)$-dimensional space Ψ spanned by the number states $|0\rangle$, $|1\rangle, \ldots, |s\rangle$. The Hermitian phase operator operates on this finite space, and after all necessary expectation values have been calculated in Ψ, the value of s is allowed to tend to infinity. A complete orthonormal basis of $(s+1)$ states is defined on Ψ as

$$|\theta_m\rangle \equiv \frac{1}{\sqrt{s+1}} \sum_{n=0}^{s} \exp(\mathrm{i} n \theta_m) |n\rangle \tag{19}$$

where

$$\theta_m \equiv \theta_0 + \frac{2\pi m}{s+1} \qquad (m = 0, 1, \ldots, s). \tag{20}$$

The value of θ_0 is arbitrary and defines a particular basis set of $(s+1)$ mutually orthogonal phase states. The Hermitian phase operator is defined as

$$\hat{\phi}_\theta \equiv \sum_{m=0}^{s} \theta_m |\theta_m\rangle\langle\theta_m| \tag{21}$$

where the subscript θ indicates the dependence on the choice of θ_0. The phase states (19) are eigenstates of the phase operator (21) with the eigenvalues θ_m restricted to lie within a phase window between θ_0 and $\theta_0 + 2\pi$. The unitary phase operator $\exp(\mathrm{i}\hat{\phi}_\theta)$ is defined as the exponential function of the Hermitian operator $\hat{\phi}_\theta$. This operator acting on the eigenstate $|\theta_m\rangle$ gives the eigenvalue $\exp(\mathrm{i}\theta_m)$, and can be written as [14–16]

$$\exp(\mathrm{i}\hat{\phi}_\theta) \equiv \sum_{n=0}^{s-1} |n\rangle\langle n+1| + \exp\left[\mathrm{i}(s+1)\theta_0\right] |s\rangle\langle 0|. \tag{22}$$

It is the last term in (22) that assures the unitarity of this operator. The first sum reproduces the Susskind–Glogower phase operator in the limit $s \to \infty$.

The expectation value of the phase operator (21) in a state $|\psi\rangle$ is given by

$$\langle\psi|\hat{\phi}_\theta|\psi\rangle = \sum_{m=0}^{s} \theta_m |\langle\theta_m|\psi\rangle|^2 \tag{23}$$

where $|\langle\theta_m|\psi\rangle|^2$ gives a probability of being found in the phase state $|\theta_m\rangle$. The density of phase states is $(s+1)/2\pi$, so in the continuum limit as s tends to infinity, we can write equation (23) as

$$\langle\psi|\hat{\phi}_\theta|\psi\rangle = \int_{\theta_0}^{\theta_0+2\pi} \theta P(\theta)\,\mathrm{d}\theta \tag{24}$$

where the continuum phase distribution $P(\theta)$ is introduced by

$$P(\theta) = \lim_{s\to\infty} \frac{s+1}{2\pi} |\langle\theta|\psi\rangle|^2 \tag{25}$$

where θ_m has been replaced by the continuous phase variable θ. As the phase distribution function $P(\theta)$ is known, all the quantum mechanical phase expectation values can be calculated with this function in a classical-like manner. The choice of the value of θ_0 defines the 2π range window of the phase values.

In our case of second harmonic generation, the state of the field (14) is in fact a two-mode state, and the generalization of the phase formalism into the two-mode case gives, for the state (14), the result

$$\begin{aligned}\langle\theta_{m_a}|\langle\theta_{m_b}|\psi(t)\rangle = {} & \frac{1}{\sqrt{(s_a+1)(s_b+1)}} \\ & \times \sum_{n=0}^{s_a} b_n \sum_{k=0}^{[n/2]} \exp\left\{-\mathrm{i}\left[(n-2k)\theta_{m_a} + k\theta_{m_b}\right]\right\} c_{n,k}(t)\end{aligned} \tag{26}$$

where we have used the indices a and b to distinguish between the fundamental (a) and second harmonic (b) mode. There is still a freedom of choice in (26) of the values of $\theta_0^{a,b}$, which define the phase values window. We have chosen these values as

$$\theta_0^{a,b} = \varphi_{a,b} - \frac{\pi s_{a,b}}{s_{a,b}+1} \tag{27}$$

and we have introduced the new phase values

$$\theta_{\mu_{a,b}} = \theta_{m_{a,b}} - \varphi_{a,b} \tag{28}$$

where the new phase labels $\mu_{a,b}$ run in unit steps between the values $-s_{a,b}/2$ and $s_{a,b}/2$. This means that we have symmetrized the phase windows for the fundamental and second harmonic modes with respect to the phases φ_a and φ_b, respectively. On inserting (27) and (28) into (26), taking the modulus square of (26), and performing the continuum limit transition, we arrive at the continuous joint probability distribution for the continuous phase variables θ_a and θ_b, which has the form

$$P(\theta_a, \theta_b) = \frac{1}{(2\pi)^2} \left| \sum_{n=0}^{\infty} b_n \mathrm{e}^{-\mathrm{i}n\varphi_a} \sum_{k=0}^{[n/2]} \exp\{-\mathrm{i}[(n-2k)\theta_a + k\theta_b - k(2\varphi_a - \varphi_b)]\} c_{n,k}(t) \right|^2 . \tag{29}$$

The distribution (29) is normalized such that

$$\int_{-\pi}^{\pi} \int_{-\pi}^{\pi} P(\theta_a, \theta_b)\, \mathrm{d}\theta_a\, \mathrm{d}\theta_b = 1. \tag{30}$$

To choose the phase windows for θ_a and θ_b, we have to assign to φ_a and φ_b particular values. It is interesting to notice that formula (29) depends, in fact, on the difference $2\varphi_a - \varphi_b$, which reproduces the classical phase relation for the second harmonic generation (we assume here perfect phase matching conditions for the wave vectors, $\Delta \boldsymbol{k} = 0$, [3]). Classically, if there is no second harmonic initially, this quantity must be $2\varphi_a - \varphi_b = \pm\pi/2$. This means that the phase of the second harmonic is locked to the phase of the fundamental mode by this relation. It turns out that this is also a good choice to fix the phase windows in the quantum description. If the initial phase φ_a of the fundamental mode is zero then $\varphi_b = \pm\pi/2$ (depending on the sign of g), i.e., the second harmonic is shifted in phase by $\pi/2$ or $-\pi/2$ with respect to the fundamental mode.

The joint probability distribution given by equation (29) can be evaluated numerically if the mean number of photons $N_a = |\alpha|^2$ of the fundamental mode is not too big. An example of such distribution is shown in figure 6, where the function $P(\theta_a, \theta_b)$ is plotted in the three-dimensional format for various values of the scaled time $\tau = \sqrt{2N_a}gt$ and $N_a = 16$. Initially the distribution is peaked at $\theta_a = 0$ in the θ_a direction reproducing the phase distribution of the coherent state of the fundamental mode, and it is completely flat in the θ_b direction representing the uniform phase distribution of the vacuum of the second harmonic mode. For $\tau = 1$, the well resolved peak of the distribution is visible, which means the relatively well defined phase of the second harmonic. The fact that this peak appears for $\theta_a = \theta_b = 0$ corroborates the classical phase relation $2\varphi_a - \varphi_b = \pi/2$, which has been assumed here to fix the phase window. For $\tau = 2$, when the intensity of the second harmonic is close to its maximum (see figure 1) the phase distribution $P(\theta_a, \theta_b)$ splits into two peaks. This splitting means a qualitative change in phase properties of the field, and it can be related with the transition in the evolution from the harmonic

generation regime into the down-conversion regime. The two-peak phase structure of the ideal squeezed states has been indicated by Vaccaro and Pegg [19], and for the down-conversion process with quantum pump by Gantsog *et al* [20]. The splitting of the phase distribution into two peaks resembles the splitting of the Q function for the fundamental mode discussed recently by Nikitin and Masalov [9]. The multi-peak structure of the Q function or/and the P function may be an indication that the field becomes a superposition of macroscopically distinguishable quantum states [10–13]. When the evolution proceeds ($\tau = 3$) the two peaks of the distribution become well separated and sharp. For still longer time ($\tau = 4$) the intensity of the second harmonic (see figure 1) approaches its maximum and either of the two peaks in the phase distribution splits into two new peaks. The process comes back into the second harmonic regime, but this time with a different 'initial' state. Such 'bifurcations' of the phase distribution lead to a multi-peak structure of the phase distribution, which means more and more uniform phase distribution. For different $N_a \gg 1$ the same features of the phase distributions can be found. However, the larger N_a is the sharper the peaks are. The fact that one peak splits into just two peaks is related to the fact that the process we discuss is the two-photon process. Generally, the joint phase probability distribution carries quite a bit of information about the quantum state of the field.

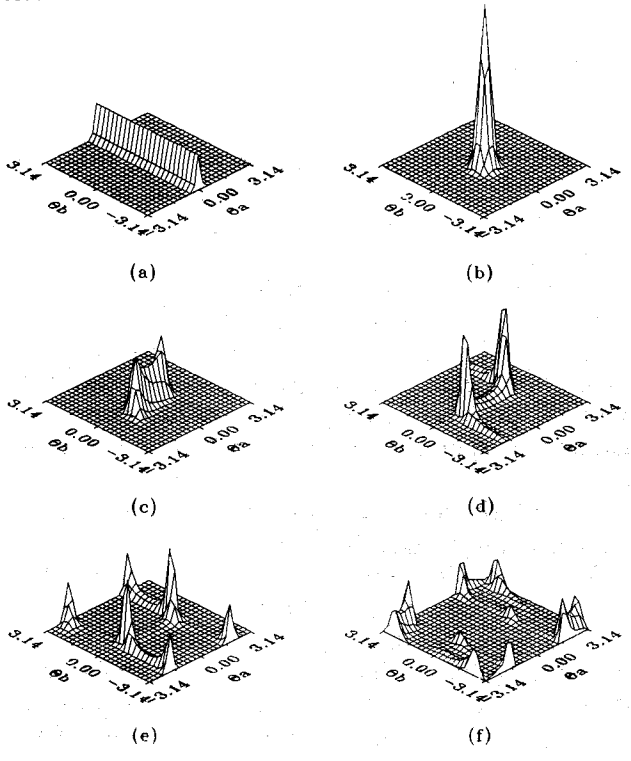

Figure 6. Evolution of the joint probability distribution $P(\theta_a, \theta_b)$, for $N_a = 16$, and: (a) $\tau = 0$, (b) $\tau = 1$, (c) $\tau = 2$, (d) $\tau = 3$, (e) $\tau = 4$, (f) $\tau = 6$.

When integration of $P(\theta_a, \theta_b)$ over one of the phases is performed, the marginal phase distributions $P(\theta_a)$ and $P(\theta_b)$ for the phases θ_a and θ_b of individual modes

are obtained. For example, we have

$$P(\theta_b) = \int_{-\pi}^{\pi} P(\theta_a, \theta_b)\,\mathrm{d}\theta_a$$
$$= \frac{1}{2\pi}\left\{1 + \sum_{n=2}\sum_{m\neq n}\sum_{l=0}^{[m/2]} |b_n||b_m| \times \exp\left[-\mathrm{i}\left(\frac{n-m}{2}\right)[\theta_b - (2\varphi_a - \varphi_b)]\right] c_{n,\frac{n-m}{2}+l}(t)c^*_{m,l}(t)\right\} \quad (31)$$

where $(n-m)/2$ must be integer. Again, we assume $2\varphi_a - \varphi_b = \pi/2$. With this condition and the property of the coefficients $c_{n,k}(t)$, which are real for k even and imaginary for k odd, the marginal distribution $P(\theta_b)$ becomes an even function of θ_b, and it can be written as

$$P(\theta_b) = \frac{1}{2\pi}\left[1 + 2\sum_{n>m}\sum_{k=0}^{[m/2]} |b_n||b_m| \times \cos\left(\frac{n-m}{2}\theta_b\right) \mathrm{Re}\left[(\mathrm{i})^{\frac{n-m}{2}} c_{n,\frac{n-m}{2}+k}(t)c^*_{m,k}(t)\right]\right]. \quad (32)$$

Similarly, for the marginal distribution $P(\theta_a)$ we get the formula

$$P(\theta_a) = \frac{1}{2\pi}\left(1 + 2\sum_{n>m}\sum_{k=0}^{[m/2]} |b_n||b_m| \cos\left[(n-m)\theta_a\right] c_{n,k}(t)c^*_{m,k}(t)\right) \quad (33)$$

which is an even function of θ_a, and the product of the $c_{n,k}(t)$ coefficients is always real.

The marginal phase distribution (32) and (33) can be used for calculations of any phase properties of the individual mode (fundamental or second harmonic). We have, for example, the following expressions for the mean values and variances of the individual modes

$$\langle\hat{\phi}_{\theta_{a,b}}\rangle = \varphi_{a,b} + \int_{-\pi}^{\pi} \theta_{a,b} P(\theta_{a,b})\,\mathrm{d}\theta_{a,b} = \varphi_{a,b} \quad (34)$$

$$\left\langle\left(\Delta\hat{\phi}_{\theta_{a,b}}\right)^2\right\rangle = \langle\hat{\phi}^2_{\theta_{a,b}}\rangle - \langle\hat{\phi}_{\theta_{a,b}}\rangle^2 = \int_{-\pi}^{\pi} \theta^2_{a,b} P(\theta_{a,b})\mathrm{d}\theta_{a,b} \quad (35)$$

where the subscripts a and b are used to distinguish between the fundamental and the second harmonic modes. Since the functions $P(\theta_a)$ and $P(\theta_b)$ are even functions of their arguments the integrals in (34) are zero. This is true under the assumption that $2\varphi_a - \varphi_b = \pi/2$, which we have made. The mean values of the phases, given by (34), remain unchanged and reproduce the classical phase relations for the second harmonic generation. Quantum mechanically, however, there are definite uncertanties

in the phase measurements, which are given by the variances (35). The integrals are elementary, and give the results

$$\langle(\Delta\hat{\phi}_{\theta_b})^2\rangle = \frac{\pi^2}{3} + 4\sum_{n>m}\sum_{k=0}^{[m/2]} |b_n||b_m| \frac{(-1)^{\frac{n-m}{2}}}{\left(\frac{n-m}{2}\right)^2} \mathrm{Re}\left[(\mathrm{i})^{\frac{n-m}{2}} c_{n,\frac{n-m}{2}+k}(t) c^*_{m,k}(t)\right] \tag{36}$$

$$\langle(\Delta\hat{\phi}_{\theta_a})^2\rangle = \frac{\pi^2}{3} + 4\sum_{n>m}\sum_{k=0}^{[m/2]} |b_n||b_m| \frac{(-1)^{n-m}}{(n-m)^2} c_{n,k}(t) c^*_{m,k}(t). \tag{37}$$

The evolution of the phase variances (36) and (37) is shown in figures 7 and 8. In the case of fundamental mode the phase variance starts from low (but non-zero) values characteristic of the coherent states, initially increases slowly, and around $\tau = 2$ rapidly increases. The broken line marks the value $\pi^2/3$ of the randomly distributed phase. Appearance of the phase variance values above $\pi^2/3$ can be explained by the choice of the phase window, which is not proper in this interval of τ (compare the phase distribution in figure 6). In the long time limit the phase variance oscillates approaching the value $\pi^2/3$, i.e., the value for randomly distributed phase. This is consistent with the joint phase distribution, which becomes more uniform because of the multi-peak structure arising during the evolution. More interesting is the behaviour of the phase variance of the second harmonic mode shown in figure 8. The variance falls rapidly from the vacuum value to some small (but non-zero) values, remains in the region of small fluctuations for some time, and next rapidly increases. This rapid increase of phase fluctuations is associated with the transition from the one-peak to the two-peak structure of the phase distribution (figure 6), and physically with the transition from the second harmonic to the down-conversion regime. It is seen that the reduction of the phase fluctuations in the second harmonic mode is more pronounced for larger N_a values. In the long time limit the randomization of the phase takes place, as for the fundamental mode.

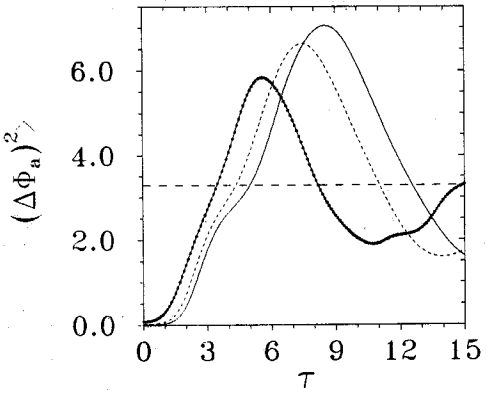

Figure 7. Evolution of the phase variance of the fundamental mode.

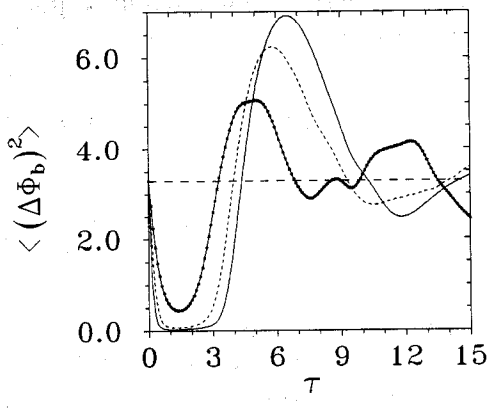

Figure 8. Same as figure 7 but for the second harmonic mode.

It is interesting to ask to what extent can the phase fluctuations be reduced in the second harmonic generation. To answer this question we compare in figure 9 the marginal distribution $P(\theta_b)$ for the minimum of the variance with the distribution $P(\theta_b)$ for the coherent state with the mean number of photons $\langle n_b \rangle$ at this minimum. It is seen that $P(\theta_b)$ is broader than the corresponding coherent state distribution. It becomes closer to the coherent state distribution when N_a becomes larger. Recently, Summy and Pegg [21] have discussed the problem of minimizing phase variance, showing the possibility of getting states with the phase defined much more sharply than that of a coherent state with the same mean energy. In the second harmonic generation with an initially coherent state, the best phase distribution one can get is that of the coherent state.

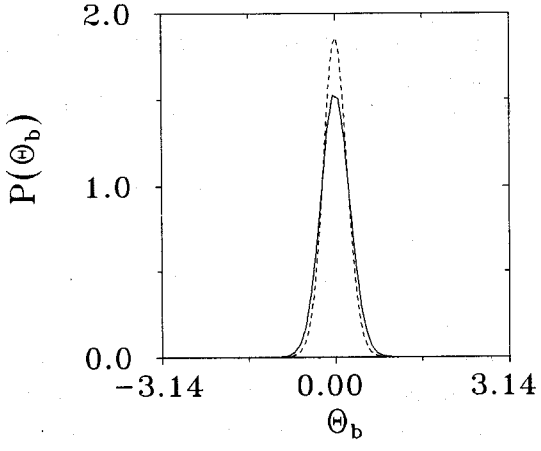

Figure 9. Comparison of $P(\theta_b)$ (full curve) at the minimum of phase fluctuations with $P(\theta_b)$ for the coherent state (broken curve) with the same mean number of photons, for $N_a = 16$ and $\tau = 1.3$.

Since the state (14) of the field is a 'physical state' according to the definition introduced by Pegg and Barnett [16], there are some useful relations between the Pegg–Barnett sine and cosine functions of the phase operators and their counterparts in the Susskind–Glogower [22,23] phase formalism. For example, for 'physical states', we have [19]

$$\langle \exp(\mathrm{i}m\hat{\phi}_\theta)\rangle_p = \left\langle \left[\sum_{n=0}^{\infty} |n\rangle\langle n+m| \right] \right\rangle_p = \langle \widehat{\exp}(\mathrm{i}m\phi_{\mathrm{SG}})\rangle_p \tag{38}$$

where the subscript p refers to a physical state expectation value. Applying the state (14), we get

$$\begin{aligned} \langle \psi(t)|\exp(\mathrm{i}m\hat{\phi}_{\theta_a})|\psi(t)\rangle &= \sum_{n=0}^{\infty} \langle \psi(t)|\left[|n\rangle\langle n+m|\right]_a|\psi(t)\rangle \\ &= \sum_n b_{n+m} b_n^* \sum_{k=0}^{[n/2]} c_{n+m,k}(t) c_{n,k}^*(t) \end{aligned} \tag{39}$$

and similarly

$$\langle\psi(t)|\exp(\mathrm{i}m\hat{\phi}_{\theta_b})|\psi(t)\rangle = \sum_n b_{n+2m}b_n^* \sum_{k=0}^{[n/2]} c_{n+2m,k+m}(t)c_{n,k}^*(t). \tag{40}$$

This gives

$$\begin{Bmatrix} \langle\cos\hat{\phi}_{\theta_a}\rangle \\ \langle\sin\hat{\phi}_{\theta_a}\rangle \end{Bmatrix} = \begin{Bmatrix} \cos\varphi_a \\ \sin\varphi_a \end{Bmatrix} \sum_n |b_{n+1}||b_n| \sum_{k=0}^{[n/2]} c_{n+1,k}(t)c_{n,k}^*(t) \tag{41}$$

$$\begin{Bmatrix} \langle\cos^2\hat{\phi}_{\theta_a}\rangle \\ \langle\sin^2\hat{\phi}_{\theta_a}\rangle \end{Bmatrix} = \tfrac{1}{2} \pm \tfrac{1}{2}\cos 2\varphi_a \sum_n |b_{n+2}||b_n| \sum_{k=0}^{[n/2]} c_{n+2,k}(t)c_{n,k}^*(t). \tag{42}$$

Corresponding relations for the second harmonic mode can be obtained from (40), bearing in mind that $2\varphi_a - \varphi_b = \pi/2$.

A more general expression than (39) and (40) can be obtained in the same way

$$\langle\exp[\mathrm{i}(m\hat{\phi}_{\theta_a} - l\hat{\phi}_{\theta_b})]\rangle = \sum_{\substack{n \\ (n+m-2l\geqslant 0)}} b_{n+m-2l}b_n^* \sum_{\substack{k=0 \\ (k-l\geqslant 0)}}^{[n/2]} c_{n+m-2l,k-l}(t)c_{n,k}^*(t). \tag{43}$$

This expression becomes particularly simple for $m = 2l$, and once more the characteristic, for the second harmonic generation, phase relation is privileged. From equation (43) the expectation values and variances of the sine and cosine functions of the difference $2\hat{\phi}_{\theta_a} - \hat{\phi}_{\theta_b}$ can be obtained. For $m = 2$ and $l = 1$ expression (43) is imaginary, which means that

$$\begin{aligned} &\langle\cos(2\hat{\phi}_{\theta_a} - \hat{\phi}_{\theta_b})\rangle = 0 \\ &\langle\sin(2\hat{\phi}_{\theta_a} - \hat{\phi}_{\theta_b})\rangle = -\mathrm{i}\langle\exp[\mathrm{i}(2\hat{\phi}_{\theta_a} - \hat{\phi}_{\theta_b})]\rangle. \end{aligned} \tag{44}$$

For $m = 4$ and $l = 2$ expression (43) is real and we get

$$\begin{Bmatrix} \langle\cos^2(2\hat{\phi}_{\theta_a} - \hat{\phi}_{\theta_b})\rangle \\ \langle\sin^2(2\hat{\phi}_{\theta_a} - \hat{\phi}_{\theta_b})\rangle \end{Bmatrix} = \tfrac{1}{2} \pm \tfrac{1}{2}\sum_n |b_n|^2 \sum_{k=2}^{[n/2]} c_{n,k-2}(t)c_{n,k}^*(t). \tag{45}$$

Formulae (39)–(47) allow for calculations of the sine and cosine functions and their variances for any combination of the two phases $\hat{\phi}_{\theta_a}$ and $\hat{\phi}_{\theta_b}$. Examples are shown in figures 10 and 11, where the evolution of the mean value of $\sin(2\hat{\phi}_{\theta_a} - \hat{\phi}_{\theta_b})$ and its variance are plotted. These two quantities can be compared to the variance of $2\hat{\phi}_{\theta_a} - \hat{\phi}_{\theta_b}$ itself, which can be calculated according to the formula

$$\langle[\Delta(2\hat{\phi}_{\theta_a} - \hat{\phi}_{\theta_b})]^2\rangle = 4\langle(\Delta\hat{\phi}_{\theta_a})^2\rangle + \langle(\Delta\hat{\phi}_{\theta_b})^2\rangle - 4[\langle\hat{\phi}_{\theta_a}\hat{\phi}_{\theta_b}\rangle - \langle\hat{\phi}_{\theta_a}\rangle\langle\hat{\phi}_{\theta_b}\rangle]. \tag{46}$$

The phase correlation function can be calculated according to

$$C_{\theta_a,\theta_b} = \langle\hat{\phi}_{\theta_a}\hat{\phi}_{\theta_b}\rangle - \langle\hat{\phi}_{\theta_a}\rangle\langle\hat{\phi}_{\theta_b}\rangle = \int_{-\pi}^{\pi}\int_{-\pi}^{\pi} \theta_a\theta_b P(\theta_a,\theta_b)\,\mathrm{d}\theta_a\,\mathrm{d}\theta_b \tag{47}$$

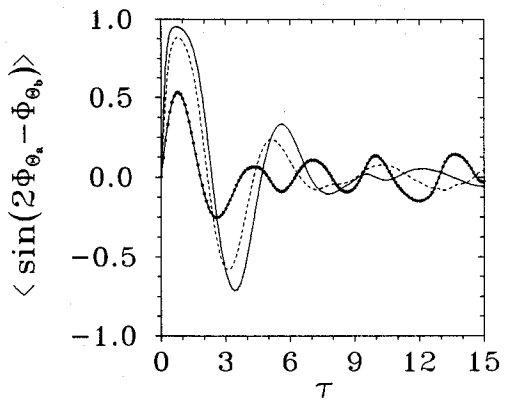

Figure 10. Evolution of $\langle \sin(2\hat{\phi}_{\theta_a} - \hat{\phi}_{\theta_b}) \rangle$.

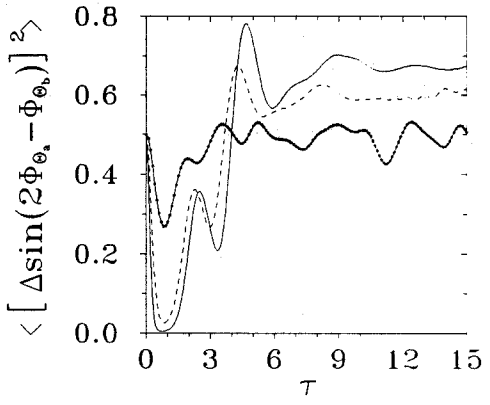

Figure 11. Evolution of the variance $\langle \sin^2(2\hat{\phi}_{\theta_a} - \hat{\phi}_{\theta_b}) \rangle - \langle \sin(2\hat{\phi}_{\theta_a} - \hat{\phi}_{\theta_b}) \rangle^2$.

and is essentially two-mode phase characteristic of the field. In figure 12 the variance of $2\hat{\phi}_{\theta_a} - \hat{\phi}_{\theta_b}$ is plotted against τ. Comparison of figures 10–12 shows that for the values of τ when the phase difference is well defined the sine is also well defined, and the mean value of the sine is close to unity, which agrees with $\langle 2\hat{\phi}_{\theta_a} - \hat{\phi}_{\theta_b} \rangle = 2\varphi_a - \varphi_b = \pi/2$.

In figure 13 the evolution of the intermode phase correlation given by equation (47) is plotted. There is a region of small negative correlations initially, a region of no correlations, and next a region of positive correlations. Essential positive phase correlations go in step with strong negative correlations of the photon numbers (figure 4) and appear after transition into the down-conversion regime.

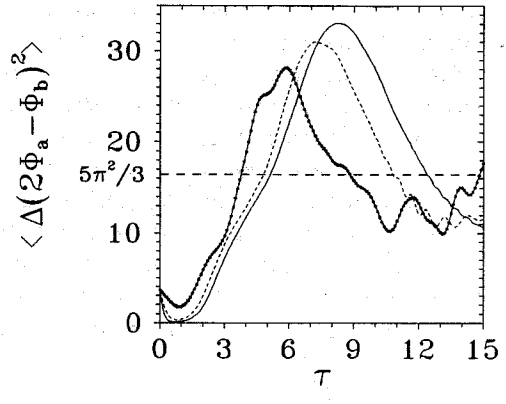

Figure 12. Evolution of the variance of $2\hat{\phi}_{\theta_a} - \hat{\phi}_{\theta_b}$.

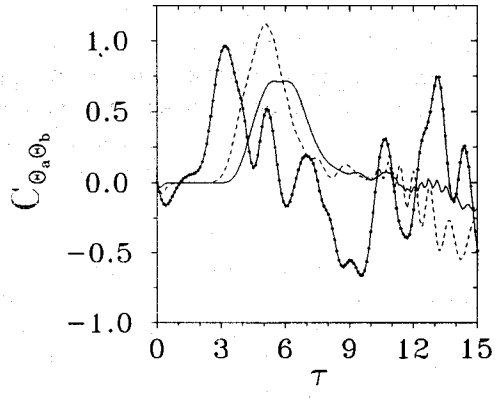

Figure 13. Evolution of the intermode phase correlation function.

Finally, in figure 14 the product of the number and phase uncertainties for the fundamental mode is plotted against τ. We have divided the number fluctuations

by N_a in order to keep all numbers on a reasonable scale. There is a region of small uncertainties initially, as it should be for a coherent state for which the product plotted in figure 14 should be of the order of $(4N_a)^{-1}$. The transition into the high level of uncertainties, which is associated with the change in the character of the process, is clearly visible.

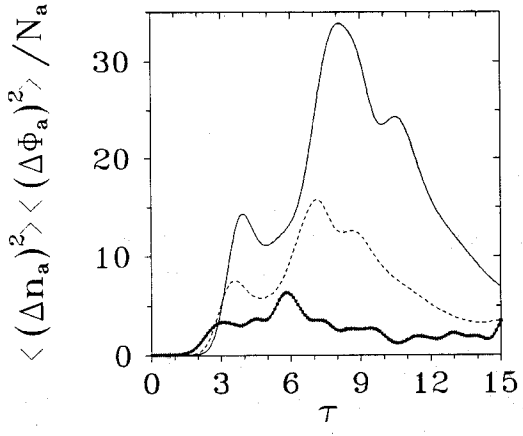

Figure 14. Evolution of the number–phase uncertainties product divided by N_a, for the fundamental mode.

5. Conclusions

We have studied the number and phase quantum fluctuations in the second harmonic generation process. The method of numerical diagonalization of the interaction Hamiltonian has been used to find the evolution of the system. The new Pegg–Barnett Hermitian phase formalism has been applied for studying phase fluctuations and correlations. It has been shown that the joint phase probability distribution undergoes a sequence of 'bifurcations' that lead into a multi-peak structure of the phase distribution. The splitting of the phase distribution function clearly indicates the transition of the process from the second harmonic into the down-conversion regime. So, the phase distribution is a new representation of the quantum state of the field, which carries a lot of essential information about this state and is now available due to the Pegg–Barnett formalism. The phase information has been compared with the number fluctuations and correlations in the two modes. The transition from a low to a high level of fluctuations is observed for both the number and phase fluctuations, although it is much more spectacular when the evolution of the phase distribution is watched.

The evolution of the phase variances for both modes has been obtained and illustrated graphically. The narrowing of the phase distribution for the second harmonic mode is clearly visible, but the marginal distribution $P(\theta_b)$ remains broader than the distribution for a coherent state with the same mean number of photons.

The cosine and sine functions of the individual phases as well as their combinations have also been calculated. It has been shown that the difference $2\hat{\phi}_{\theta_a} - \hat{\phi}_{\theta_b}$,

which is specific for the second harmonic generation, has a specific form, and confirms the classical phase relation for this process. There are, however, quantum phase fluctuations that spoil this relation.

Most of our results are presented for three different values of the mean number of photons of the initially coherent fundamental mode ($N_a = 4$, 16, and 36). These numbers are taken so to satisfy the condition $N_a \gg 1$, and as they increase, they clearly show the tendency for changes in the strong field limit.

In the long time limit the phases of both modes are randomized, i.e. their distribution becomes more and more uniform owing to the multi-peak structure that appears during the evolution. The second harmonic generation in its pure form takes place only at the initial stage of the process, and at later stages there is a competition between the second harmonic generation and the down-conversion processes, and the phase distribution clearly detects the transition between the two.

References

[1] Franken P A, Hill A E, Peters C W and Weinreich G 1961 *Phys. Rev. Lett.* **7** 118
[2] Kielich S 1981 *Nonlinear Molecular Optics* (Moscow: Nauka)
[3] Shen Y R 1985 *The Principles of Nonlinear Optics* (New York: Wiley)
[4] Walls D F and Tindle 1971 *Nuovo Cimento Lett.* **2** 915; 1972 *J. Phys. A: Gen. Phys.* **8** 534
[5] Kozierowski M and Tanaś R 1977 *Opt. Commun.* **21** 229
[6] Mandel L 1982 *Opt. Commun.* **42** 437
[7] Wu L, Kimble H J, Hall J L and Wu H 1986 *Phys. Rev. Lett.* **57** 2520
[8] Kielich S, Kozierowski M and Tanaś R 1985 *Opt. Acta* **32** 1023
[9] Nikitin S P and Masalov A V 1991 *Quantum Opt.* **3** 105
[10] Yurke B and Stoler D 1986 *Phys. Rev. Lett.* **57** 13
[11] Miranowicz A, Tanaś R and Kielich S 1990 *Quantum Opt.* **2** 253
[12] Gantsog Ts and Tanaś R 1991 *J. Mod. Opt.* **38** in press
[13] Gantsog Ts and Tanaś R 1991 *Quantum Opt.* **1** 33
[14] Pegg D T and Barnett S M 1988 *Europhys. Lett.* **6** 483
[15] Barnett S M and Pegg D T 1989 *J. Mod. Opt.* **36** 7
[16] Pegg D T and Barnett S M 1989 *Phys. Rev.* A **39** 1665
[17] Walls D F and Barakat R 1970 *Phys. Rev.* A **1** 446
[18] Mostowski J and Rzążewski K 1978 *Phys. Lett.* **66A** 275
[19] Vaccaro J A and Pegg D T 1989 *Opt. Commun.* **70** 529
[20] Gantsog Ts, Tanaś R and Zawodny R 1991 *Opt. Commun.* **82** 345
[21] Summy S S and Pegg D T 1990 *Opt. Commun.* **77** 75
[22] Susskind L and Glogower J 1964 *Physics* **1** 49
[23] Carruthers P and Nieto M M 1968 *Rev. Mod. Phys.* **40** 411